INTERNATIONAL JOURNAL OF MOLECULAR MEDICINE 34: 1124-1132, 2014

Modulation of gene expression in endothelial cells in response to high LET nickel ion irradiation

MICHAËL BECK[1,2], CHARLOTTE ROMBOUTS[1,2], MARJAN MOREELS[1], AN AERTS[1], ROEL QUINTENS[1], KEVIN TABURY[1], ARLETTE MICHAUX[1], ANN JANSSEN[1], MIEKE NEEFS[1], ERIC ERNST[3], BIRGER DIERIKS[2,4], RYONFA LEE[5], WINNOK H. DE VOS[2,4,6], CHARLES LAMBERT[3], PATRICK VAN OOSTVELDT[2,4] and SARAH BAATOUT[1,2]

[1]Laboratory of Radiobiology, Institute for Environment, Health and Safety, Belgian Nuclear Research Centre (SCK-CEN), Mol; [2]Department of Molecular Biotechnology, Ghent University, Ghent; [3]Laboratory of Connective Tissues Biology, GIGA-Cancer, University of Liège, Liège; [4]NB-Photonics, Ghent University, Ghent, Belgium; [5]Biophysics Department, GSI Helmholtzzentrum für Schwerionenforschung, Darmstadt, Germany; [6]Laboratory of Cell Biology and Histology, Department of Veterinary Sciences, Antwerp University, Antwerp, Belgium

Received February 9, 2014; Accepted May 6, 2014

DOI: 10.3892/ijmm.2014.1893

Abstract. Ionizing radiation can elicit harmful effects on the cardiovascular system at high doses. Endothelial cells are critical targets in radiation-induced cardiovascular damage. Astronauts performing a long-term deep space mission are exposed to consistently higher fluences of ionizing radiation that may accumulate to reach high effective doses. In addition, cosmic radiation contains high linear energy transfer (LET) radiation that is known to produce high values of relative biological effectiveness (RBE). The aim of this study was to broaden the understanding of the molecular response to high LET radiation by investigating the changes in gene expression in endothelial cells. For this purpose, a human endothelial cell line (EA.hy926) was irradiated with accelerated nickel ions (Ni) (LET, 183 keV/μm) at doses of 0.5, 2 and 5 Gy. DNA damage was measured 2 and 24 h following irradiation by γ-H2AX foci detection by fluorescence microscopy and gene expression changes were measured by microarrays at 8 and 24 h following irradiation. We found that exposure to accelerated nickel particles induced a persistent DNA damage response up to 24 h after treatment. This was accompanied by a downregulation in the expression of a multitude of genes involved in the regulation of the cell cycle and an upregulation in the expression of genes involved in cell cycle checkpoints. In addition, genes involved in DNA damage response, oxidative stress, apoptosis and cell-cell signaling (cytokines) were found to be upregulated. An *in silico* analysis of the involved genes suggested that the transcription factors, E2F and nuclear factor (NF)-κB, may be involved in these cellular responses.

Correspondence to: Professor Sarah Baatout, Laboratory of Radiobiology, Molecular and Cellular Biology Expert Group, Institute for Environment, Health and Safety, Belgian Nuclear Research Centre (SCK-CEN), Boeretang 200, 2400 Mol, Belgium
E-mail: sarah.baatout@sckcen.be

Key words: gene expression, radiation, high-linear energy transfer, cardiovascular system, endothelial cells

Introduction

Cardiovascular disease is considered to be one of the most important non-cancer long-term effects of ionizing radiation, as evidenced by the epidemiological data of atomic bomb survivors exposed to doses of 0.5 to 2 Gy (1). In the context of space exploration, high linear energy transfer (LET) radiation found in space produces high values of relative biological effectiveness (RBE), as compared to low LET radiation, such as X-rays or gamma-rays, which can increase the health risks to astronauts (2). Indeed, during long-term missions, such as a journey to Mars, astronauts are bound to be exposed to cumulative doses between 0.3 and 4 Sv, depending on the spacecraft shielding and on the intensity of solar particle events (3).

Heavy ion irradiation is also used for terrestrial applications, such as non-conventional radiotherapy (hadron therapy), which takes advantage of the depth distribution of the dose, which is maximal at the Bragg peak, and of the increased RBE, allowing the enhanced killing effect on tumor cells while sparing the healthy tissue (4,5). However, little is known of the molecular mechanisms involved in the enhanced killing properties of heavy ion irradiation. Improving our understanding of the effects of heavy ion radiation, particularly on the cardiovascular system that may be irradiated during treatment, is therefore of utmost importance for both long-term space missions and hadron therapy.

Endothelial cells are critical targets in radiation-induced cardiovascular damage (1,6,7). While high doses of low LET radiation induce pro-inflammatory responses in endothelial cells, the opposite has been observed upon exposure to low doses (8-10). The mechanisms involved are not yet fully understood; however, they appear to be at least partly linked

to the transcription factor, nuclear factor (NF)-κB, and the nitric oxide signaling pathway, which in turn mediates various cellular responses, including the secretion of cytokines [such as transforming growth factor (TGF)-β1, interleukin (IL)-6, interferon (IFN)-γ, IFN-β and tumor necrosis factor (TNF)-α] and chemokines (9-11). Another possible mechanism of radiation-induced cardiovascular alteration, as shown upon low LET radiation (12-16), is the endothelial retraction and the impairment of cellular adhesion. Matrix metalloproteinases (MMPs), Rho GTPases, calcium signaling and reactive oxygen species seem to be important factors that stimulate modifications in cell junctions and the cytoskeleton through adhesion molecules and actin (12-16). Although high LET radiation has been shown to reduce the length of a 3D human endothelial vessel model, both developing and mature (17), only a few studies have been conducted to identify the mechanisms involved in the endothelial response to high LET radiation (18,19).

Thus, the aim of this study was to investigate the effects of moderate and high doses of high LET nickel ion (Ni) irradiation on gene expression in endothelial cells in order to elucidate the molecular mechanisms responsible for radiation-induced cardiovascular damage. For this purpose, the EA.hy926 cell line, which originates from human umbilical vein endothelial cells, was irradiated with nickel ions (LET, 183 keV/μm) at moderate (0.5 Gy) and high (2 and 5 Gy) doses after which gene expression was determined by whole-genome microarray analysis.

Materials and methods

Cell culture. The human EA.hy926 endothelial cells were obtained from the American Type Culture Collection (ATCC; Manassas, VA, USA). They were cultured (37˚C-5% CO_2) in Dulbecco's modified Eagle's medium supplemented with 10% fetal bovine serum and 1% penicillin/streptomycin (all from N.V. Invitrogen S.A., Merelbeke, Belgium). The cells were regularly examined for the absence of mycoplasma using the LookOut® Mycoplasma PCR Detection kit (Sigma-Aldrich, St. Louis, MO, USA).

Nickel irradiation. The cells were seeded at a density of 10^5 cells in 12.5 cm^2 flasks. Twenty-four hours after plating, the flasks were placed in a transportable incubator (37˚C) and moved from the resident laboratory (Mol, Belgium) to the GSI Helmholtzzentrum für Schwerionenforschung GmbH (Darmstadt, Germany). Forty-eight hours after plating, the subconfluent cells were irradiated in flasks completely filled with culture medium with a 1 GeV/u Ni beam at the SIS facility at GSI with the intensity controlled raster scanning technique as described by Haberer *et al* (20). The ion energy at the sample position was approximately 930 MeV/u with a LET of 183 keV/μm (calculated with the program code ATIMA). The culture flasks were placed vertically and exposed perpendicularly to the nickel ion beam at the following doses: 0.5, 2 and 5 Gy. Non-irradiated control samples were treated similarly to the irradiated samples, but placed out of the beam. Following irradiation, the cells were incubated (37˚C, 5% CO_2) in 2 ml of conditioned medium until fixation time points (2, 8 and 24 h).

DNA double-strand break detection (detection of γ-H2AX foci). The cells were fixed in 4% paraformaldehyde (Merck KGaA, Darmstadt, Germany) 2 and 24 h after irradiation. They were then treated with 0.25% Triton X for 5 min, blocked with 3% bovine serum albumin (both from Sigma-Aldrich) for 30 min and incubated overnight with mouse anti-γ-H2AX antibody (Abcam, Cambridge, MA, USA) at 4˚C. After a second blocking of 10 min, the cells were incubated for 1 h with anti-mouse secondary antibody coupled to FITC (Sigma-Aldrich) at 37˚C and then mounted in Vectashield mounting medium (Vector Laboratories, Burlingame, CA, USA) with DAPI. Between each of the previous steps, the slides were washed with phosphate-buffered saline (PBS).

An automated inverted fluorescence microscope (TE2000-E; Nikon, Tokyo, Japan), equipped with a motorized XYZ stage, emission and excitation filter wheels, shutters and a triple dichroic mirror (436/514/604) was used for the image acquisition of the immunostained slides. Images were acquired with a 40X Plan Fluor oil objective (NA 1.3) and an Andor iXon EMCCD camera (Andor Technology, South Windsor, CT, USA). For each sample, at least 12 fields were acquired on 5 z-stack focusses (1 μm). The γ-H2AX spot number and spot occupancy were analyzed with the INSCYDE plugin for ImageJ as previously described (21). Spot occupancy was defined for each nucleus as the sum of the spot areas divided by the nucleus area (spot_occupancy = sum (spot_area)/ nuclear_area). A minimum number of 100 cells was analyzed in 2 biological replicates per condition. For statistical analyses, the data were analyzed using the Mann-Whitney U test with SPSS version 17.0 software (IBM Corp., Chicago, IL, USA) and box plots were generated using the same software. P-values <0.05 were considered to indicate statistically significant differences.

RNA extraction. At 2 time points after irradiation (8 and 24 h), the adherent cells were washed in PBS, lysed in 350 ml of AllPrep DNA/RNA/Protein Mini kit lysis buffer (Qiagen, Hilden, Germany) and frozen at -80˚C. RNA was extracted using the same kit and its concentration was measured using a NanoDrop spectrophotometer (Thermo Fisher Scientific, Waltham, MA, USA), while its quality (RNA integrity number, RIN) was determined using Agilent's lab-on-chip Bioanalyzer 2100 (Agilent Technologies, Santa Clara, CA, USA). All RNA samples had a RIN value >9.0.

Affymetrix microarrays and data analysis. RNA was processed using the GeneChip WT cDNA Synthesis and Amplification kit (Affymetrix, Santa Clara, CA, USA) according to the manufacturer's instructions. The resulting RNA was hybridized to Affymetrix Human Gene 1.0 ST arrays which contain an estimated number of 28,869 genes based on the March 2006 [UCSC Hg 18; National Center for Biotechnology Information (NCBI) build 36] human genome assembly. Biological triplicates were collected for each condition.

Raw data (.cel-files) were imported at exon level in Partek Genomics Suite version 6.5 (Partek, Inc., St. Louis, MO, USA). Briefly, robust multi-array average (RMA) background correction was applied, data were normalized by quantile normalization and probeset summarization was performed by the median polish method. Gene summarization was performed using one-step Tukey's biweight method. The obtained data were analyzed with Partek Genomics Suite for single gene analysis. One- or two-way ANOVA, taking into consideration

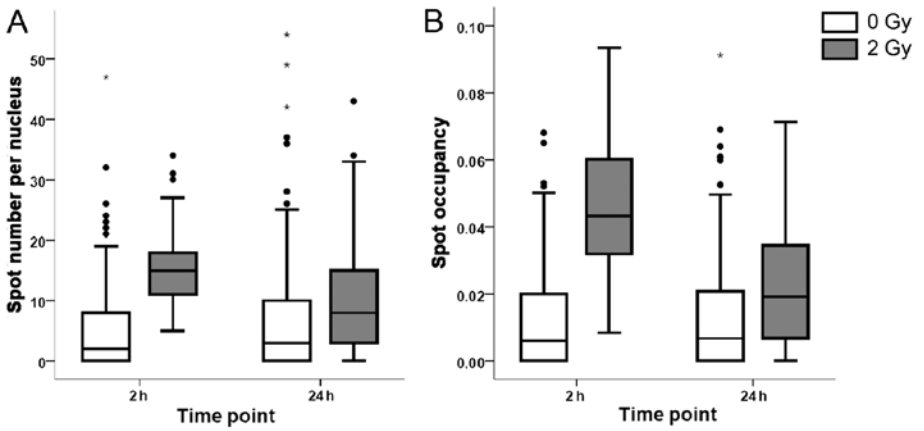

Figure 1. Box plots of the γ-H2AX (A) spot number per nucleus and (B) spot occupancy in human endothelial cells 2 and 24 h after irradiation with nickel ions (Ni). Dots represent outliers and stars represent extreme values. In both graphs, the spot number in the samples subjected to 2 Gy irradation (gray boxes) was significantly higher than the controls (0 Gy, white boxes), as shown by the Mann-Whitney U test.

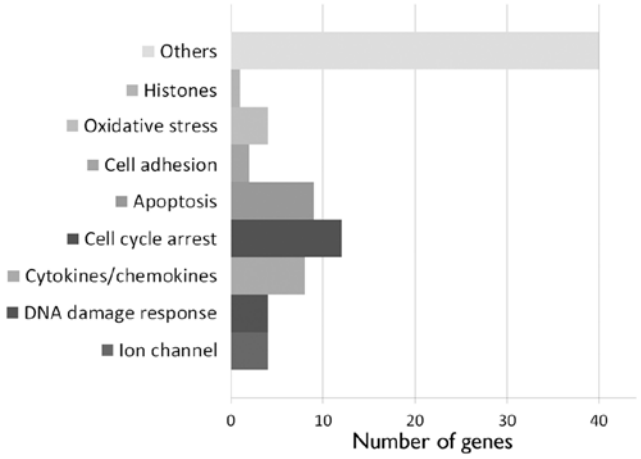

Figure 2. Number of upregulated genes in specific cellular processes 24 h after nickel ion irradiation (5 Gy). The referred processes were determined by search on the National Center for Biotechnology Information (NCBI) database.

the scan date (where applicable) and the dose as factors, were performed for each time point. In order to determine statistical significance, thresholds were set on the p-value <0.001 and on the fold-change >1.5.

The enrichment of the transcription factor binding motifs was analyzed using Pscan Ver. 1.2 (22) and the JASPAR database, scanning in a region from -950 to +50 base pairs from the transcription start site.

Results

DNA damage. To assess DNA damage induction by nickel ion irradiation and evaluate the cell capacity required to repair this damage, we performed a high content cytometric assay of γ-H2AX, 2 and 24 h after exposure. As measured by the number of γ-H2AX foci, DNA damage was significantly increased 2 h after nickel ion irradiation (2 Gy), with an average number of 15 foci per nucleus vs. 2 foci per nucleus in the control samples (Fig. 1A). Twenty-four hours after irradiation, the number of foci decreased to 9 per nucleus, which was significantly higher than the values of controls, indicating that part of the DNA damage persisted for at least 24 h. Similar trends were observed for the spot occupancy, which is the fraction of the projected area of the nucleus occupied by the signal from the γ-H2AX foci (Fig. 1B).

Effects of nickel irradiation on gene expression. In order to evaluate gene expression, we performed microarrays 8 and 24 h after irradiation. A 0.5 Gy irradiation, both after 8 and 24 h, elicited a subtle effect on gene expression in the EA.hy926 cells. Six annotated genes were differentially regulated with fold changes (FC) between 1.5 and 1.8 after 8 h, and 18 genes were differentially regulated with an FC between 1.5 and 2.3 after 24 h. A more drastic effect was observed at 5 Gy, 24 h after irradiation. At this time point, we detected the upregulation of 77 annotated genes (Fig. 2 and Table I; maximum FC, 3.4). Among these genes, cytokines and chemokines (CXCL5, TGFA, TRIM22, TNFSF9, EBI3, IL-6, IL-11 and CD70) were identified, as well as genes involved in DNA damage response (SPATA18, POLL, APOBEC3H and SESN1), cell cycle arrest (ZMAT3, MXD4, TP53INP1, HSPB8, TGFA, SESN2, BTG2, DTX3, TOB1, HBP1, CDKN1A and PLK3) and apoptosis (TP53INP1, HSPB8, TGFA, TP53I3, MOAP1, CYFIP2, TRADD, DTX3 and FAS). In addition, we observed the upregulation of genes coding for ion channels (SLC22A4, KCNJ2, ORAI3 and CLIC3), cell adhesion (CEACAM1 and NEU1) and oxidative stress response proteins (FMO4, FDXR, SIRT2 and SESN1).

A total of 145 annotated genes was downregulated 24 h after nickel ion irradiation (5 Gy) (Fig. 3 and Table I). The majority (62 genes) is known to be involved in various aspects of cell division, such as DNA replication, replication forks and chromosome assembly and segregation (Table II and Fig. 4). Other downregulated genes found have been implicated in post-replicative DNA repair (UNG, UPF3A, MSH2 and MSH6), nucleotide biosynthesis (DHFR and RRM2), DNA repair (FANCA, MMS22L, NFKBIL2, RAD51, EXO1 and HMGB2), positive (YAP1) and negative regulation of apoptosis (DHRS2, DHCR24 and MTBP), Rho signaling (ARHGAP19, ARHGAP11B and RACGAP1) and cell adhesion (PVRL1 and DLGAP5).

Table I. List of the differentially expressed genes at 8 and 24 h after 0.5 and 5 Gy of nickel ion irradiation.

Downregulated genes				Upregulated genes			
Gene symbol	GenBank	p-value	FC	Gene symbol	GenBank	p-value	FC
List of differentially expressed genes 8 h after 0.5 Gy nickel ion irradiation							
CRYBB2	NM_000496	1,02E-03	-1,800	HSP90AA6P	NR_036751	6,55E-03	1,630
GNAT1	NM_144499	5,54E-03	-1,601	RFT1	NM_052859	6,83E-03	1,572
DNAJB13	NM_153614	3,79E-03	-1,521	DEFB123	NM_153324	8,50E-03	1,518
List of differentially expressed genes 24 h after 0.5 Gy nickel-ion irradiation							
UPF3A	NM_023011	1,53E-03	-1,932	C1orf113	ENST00000312808	8,96E-03	2,224
E2F8[a]	NM_024680	5,38E-03	-1,716	SNORD53	NR_002741	6,78E-03	2,182
LIMA1	NM_001113546	9,63E-03	-1,670	SLC45A4	BC033223	8,10E-03	2,049
C16orf55	AK303024	7,00E-04	-1,600	HIST1H2BD	NM_021063	9,01E-03	2,028
HLA-DRB4	AK293020	3,18E-03	-1,583	ZNF16	NM_001029976	3,65E-03	1,952
MCM10[a]	NM_182751	9,77E-03	-1,530	RNF207	NM_207396	7,07E-03	1,677
PROK2	NM_001126128	8,29E-03	-1,518	LCE1E[b]	NM_178353	4,89E-03	1,619
				C10orf72	NM_001031746	6,04E-04	1,592
				PMCH	NM_002674	7,49E-03	1,591
				RUNDC3B	NM_138290	1,98E-03	1,571
				ORAI3[b]	NM_152288	7,01E-03	1,515
List of differentially expressed genes 24 h after 5 Gy nickel-ion irradiation							
FAM111B[a]	NM_198947	5,65E-03	-5,894	ACTA2[b]	NM_001141945	2,01E-05	3,424
PCBP1[a]	NM_006196	6,05E-04	-3,611	TP53INP1	NM_033285	1,02E-04	2,976
DHRS2	NM_182908	6,48E-05	-3,090	CD70[b]	NM_001252	9,56E-03	2,702
MCM6[a]	NM_005915	1,81E-05	-3,069	PHOSPHO1	NM_001143804	9,47E-04	2,629
HIST1H1T	NM_005323	6,99E-03	-2,762	CDKN1A	NR_037151	8,27E-03	2,221
ZNF367[a]	NM_153695	1,61E-04	-2,669	CEACAM1	NM_001712	5,56E-04	2,184
KIF20A	NM_005733	4,17E-04	-2,595	BTG2[b]	NM_006763	1,08E-03	2,170
LMNB1	NM_005573	9,94E-04	-2,561	APOBEC3H[b]	NM_001166003	4,32E-03	2,070
HIST1H1D	NM_005320	4,45E-03	-2,478	TRIM22[b]	NM_006074	4,27E-04	2,063
E2F8[a]	NM_024680	3,88E-04	-2,469	KCNJ2[b]	NM_000891	1,88E-03	2,055
HAUS8	NM_033417	1,71E-05	-2,444	SPATA18[b]	NM_145263	1,16E-06	2,026
MYBL2	NM_002466	7,56E-04	-2,369	ZNF223[b]	NM_013361	4,56E-03	1,997
UHRF1[a]	NM_001048201	5,93E-03	-2,363	LCE1E[b]	NM_178353	8,26E-04	1,986
SRP19	ENST00000512790	6,66E-03	-2,337	FDXR	NM_024417	1,72E-03	1,972
UPF3A	NM_023011	4,54E-04	-2,292	TUBA4A	NM_006000	1,36E-03	1,932
DLGAP5[a]	NM_014750	9,85E-03	-2,264	PSTPIP2	NM_024430	5,51E-04	1,924
ATAD2[a]	NM_014109	7,92E-03	-2,239	ACY3[b]	NM_080658	8,81E-03	1,922
UNG[a]	NM_003362	2,21E-05	-2,220	SLC40A1[b]	NM_014585	2,55E-03	1,921
HELLS[a]	NM_018063	8,16E-03	-2,194	TMEM150A	NM_001031738	5,23E-04	1,904
MCM3[a]	NM_002388	1,81E-03	-2,189	MXD4	NM_006454	1,09E-04	1,903
FIGNL1	NM_001042762	6,39E-03	-2,184	IL-6[b]	NM_000600	2,89E-03	1,883
KIF11	NM_004523	9,41E-03	-2,164	NCRNA00219	NR_015370	8,85E-03	1,864
FBXO5	NM_012177	1,38E-05	-2,150	KBTBD8[b]	NM_032505	8,57E-03	1,833
E2F2[a]	NM_004091	3,11E-04	-2,126	NIPAL3[b]	NM_020448	1,16E-06	1,819
WDR76	NM_024908	4,11E-04	-2,108	RAB4B	NM_016154	3,30E-03	1,811
HIST1H2BG[a]	NM_003518	1,90E-03	-2,106	SAT1[b]	NR_027783	7,52E-03	1,810
LOC1720	NR_033423	1,54E-03	-2,101	SLC22A4	NM_003059	7,67E-04	1,796
CAMK2N1	NM_018584	1,24E-03	-2,091	NEU1	NM_000434	2,68E-03	1,778
DLEU2[a]	NR_002612	6,87E-03	-2,088	CYFIP2[b]	NM_001037332	5,48E-03	1,770
MCM5[a]	NM_006739	2,95E-04	-2,084	TNFSF9	NM_003811	7,09E-04	1,736
ANKRD36B	NM_025190	3,63E-03	-2,082	TMEM217[b]	NM_145316	7,60E-03	1,730
POLA1[a]	NM_016937	2,54E-03	-2,073	IL-11	NM_000641	3,38E-03	1,721
BUB1B	NM_001211	1,55E-03	-1,995	ATP6V0A4	NM_020632	7,57E-03	1,712
GPSM2	NM_013296	2,43E-04	-1,988	FMO4	NM_002022	1,05E-03	1,707

Table I. Continued.

Downregulated genes				Upregulated genes			
Gene symbol	GenBank	p-value	FC	Gene symbol	GenBank	p-value	FC
HMGB2	NM_001130688	3,20E-03	-1,979	WIPI1	NM_017983	7,41E-04	1,705
DHCR24	NM_014762	3,24E-04	-1,970	HBP1	NM_012257	7,81E-03	1,684
MCM7[a]	NM_005916	2,60E-05	-1,956	UCN2	NM_033199	4,81E-03	1,683
ANLN	NM_018685	7,33E-03	-1,953	bEBI3	NM_005755	1,99E-03	1,676
NDC80	NM_006101	2,04E-04	-1,953	bFAS	NM_000043	9,18E-03	1,673
MCM2[a]	NM_004526	2,05E-04	-1,927	CLIC3[b]	NM_004669	8,25E-03	1,666
CDKN3	NM_005192	9,25E-03	-1,917	TGFA	NM_003236	1,70E-04	1,662
EMP2	NM_001424	1,87E-03	-1,915	NCF2[b]	NM_000433	6,46E-03	1,656
TACC3	NM_006342	2,72E-03	-1,906	NADSYN1	NM_018161	4,99E-04	1,651
LHX2	NM_004789	8,33E-03	-1,883	CXCL5[b]	NM_002994	2,65E-05	1,643
NCAPG2	NM_017760	1,59E-03	-1,881	SESN2[b]	NM_031459	8,22E-04	1,642
DHFR	NM_000791	1,91E-05	-1,878	HSPB8	NM_014365	1,53E-04	1,634
PER3[a]	NM_016831	8,02E-03	-1,867	FAM84A[b]	NM_145175	3,91E-04	1,623
SEMA3D	NM_152754	7,14E-03	-1,867	ORAI3[b]	NM_152288	3,54E-03	1,616
KIFC1	NM_002263	1,96E-04	-1,860	C9orf150[b]	NM_203403	2,10E-03	1,614
DEPDC1B	NM_018369	5,71E-03	-1,853	C2orf80	NM_001099334	5,67E-04	1,613
USP1	NM_003368	1,74E-03	-1,848	PLK3	NM_004073	8,79E-03	1,611
CCNE2	NM_057749	1,34E-03	-1,841	MAGED4[b]	NM_001098800	1,62E-03	1,611
PRC1	NM_003981	1,06E-03	-1,838	LRRC29	NM_012163	2,25E-06	1,589
DEPDC1	NM_001114120	1,89E-04	-1,819	POLL	NM_001174084	2,96E-03	1,583
ORC1	NM_004153	2,50E-03	-1,811	DFNA5	NM_004403	6,35E-04	1,578
CDCA7[a]	NM_031942	1,42E-04	-1,807	CRYAB	NM_001885	3,49E-04	1,577
MCM10[a]	NM_182751	2,11E-03	-1,801	WBP5	NM_016303	2,50E-04	1,569
CDT1[a]	NM_030928	5,55E-03	-1,800	SESN1	NM_014454	6,34E-03	1,565
FAM111A[a]	NM_022074	5,61E-04	-1,798	RDH10[b]	NM_172037	8,25E-03	1,556
STX11[a]	NM_003764	1,61E-03	-1,795	BHLHE40[b]	NM_003670	9,87E-03	1,553
MSH2[a]	NM_000251	7,76E-04	-1,794	FAM113A	AK293638	7,81E-04	1,550
MKKS	NM_018848	6,55E-04	-1,794	LOC100130581	NR_027413	6,57E-03	1,546
CEP78	NM_001098802	9,07E-03	-1,790	MOAP1	NM_022151	2,89E-04	1,543
RFC4	NM_002916	3,92E-03	-1,789	TP53I3[b]	NM_004881	1,71E-04	1,543
KIF23	NM_138555	3,79E-03	-1,789	OR51B6	NM_001004750	5,49E-03	1,542
MLF1IP[a]	NM_024629	2,81E-04	-1,785	NIPSNAP1[b]	NM_003634	3,88E-04	1,541
CEP55	NM_018131	4,87E-04	-1,782	HHAT[b]	NM_001170580	2,41E-03	1,536
TCF19[a]	NM_007109	6,78E-04	-1,781	ARR3	NM_004312	7,01E-04	1,535
BUB1	NM_004336	6,08E-04	-1,780	SIRT2[b]	NM_012237	4,30E-03	1,533
CHAF1B	NM_005441	1,22E-03	-1,773	C15orf33[b]	NM_152647	1,43E-03	1,526
EZH2[a]	NM_004456	5,38E-04	-1,772	RBKS[b]	NM_022128	5,82E-03	1,523
PLK4	NM_014264	2,16E-04	-1,757	DTX3[b]	NM_178502	4,95E-03	1,519
E2F1[a]	NM_005225	1,61E-03	-1,755	TOB1	NM_005749	6,18E-03	1,517
H1F0[a]	NM_005318	1,51E-04	-1,740	ADCY4[b]	NM_001198592	5,24E-03	1,514
CEP57L1	NM_001083535	5,12E-03	-1,739	ARL15	NM_019087	1,98E-03	1,512
NUSAP1[a]	NM_016359	8,15E-05	-1,730	TRADD[b]	NM_003789	2,41E-03	1,509
ESPL1	NM_012291	9,12E-03	-1,724	ZMAT3[b]	NM_022470	5,71E-05	1,502
KIF2C	NM_006845	7,54E-04	-1,718				
DEPDC4	NM_152317	3,25E-03	-1,714				
MSH6	NM_000179	6,14E-03	-1,712				
CDC6[a]	NM_001254	2,07E-03	-1,710				
PM20D2[a]	NM_001010853	7,65E-04	-1,706				
PVRL1	NM_002855	9,24E-03	-1,693				
C16orf55	AK303024	3,86E-04	-1,691				
RRM2[a]	NM_001165931	7,98E-03	-1,687				

Table I. Continued.

Downregulated genes				Downregulated genes			
Gene Symbol	GenBank	p-value	FC	Gene Symbol	GenBank	p-value	FC
HIST1H3F[a]	NM_021018	8,20E-03	-1,682	DDX12	NR_033399	3,55E-03	-1,570
ZNF716	NM_001159279	2,70E-04	-1,682	FLJ30064	AK054626	2,40E-03	-1,562
KIAA1524	NM_020890	1,99E-04	-1,680	USP37[a]	NM_020935	3,15E-04	-1,566
FANCA[a]	NM_000135	6,54E-06	-1,680	PLS1	NM_001172312	9,23E-04	-1,559
KLHL23	NM_144711	8,07E-03	-1,679	MT4	NM_032935	7,81E-03	-1,558
CDCA2	NM_152562	3,22E-03	-1,677	GTSE1	NM_016426	6,65E-03	-1,556
WHSC1	NM_133330	7,07E-04	-1,677	KCTD12[a]	NM_138444	7,18E-03	-1,555
MMS22L	NM_198468	2,44E-04	-1,675	ZNF749[a]	NM_001023561	3,89E-03	-1,553
FAM72D	AB096683	2,28E-03	-1,674	CENPH[a]	NM_022909	1,88E-03	-1,547
KIAA0101[a]	NM_014736	2,64E-03	-1,663	DDX11	NM_030653	7,35E-04	-1,545
AREG	NM_001657	8,49E-03	-1,658	SNX5	NM_152227	4,96E-03	-1,543
GINS2[a]	NM_016095	7,86E-03	-1,657	MTBP[a]	NM_022045	4,20E-03	-1,539
ARHGAP11B[a]	NM_001039841	1,80E-03	-1,657	GAR1	NM_018983	8,34E-03	-1,539
LYAR	NM_017816	9,45E-03	-1,656	NUF2	NM_145697	2,74E-04	-1,531
YAP1	NM_001130145	1,60E-03	-1,655	CCNF[a]	NM_001761	8,64E-04	-1,529
PKP4	NM_003628	4,89E-03	-1,653	PBK[a]	NM_018492	3,92E-03	-1,528
FGF12	NM_021032	2,85E-03	-1,649	NCAPH	NM_015341	3,03E-05	-1,521
NFKBIL2	NM_013432	2,44E-03	-1,632	EXO1[a]	NM_130398	3,35E-03	-1,521
FOXD4L3[a]	NM_199135	3,14E-03	-1,631	NOS1AP	NM_014697	7,34E-03	-1,520
CALML4	NM_033429	6,12E-03	-1,609	RACGAP1	NM_013277	6,33E-03	-1,517
DSCC1	NM_024094	2,26E-03	-1,602	CLCNKA	NM_004070	2,68E-03	-1,517
PRIM1	NM_000946	2,41E-05	-1,593	FAM133B	NM_001040057	7,16E-03	-1,515
DTL[a]	NM_016448	2,55E-04	-1,591	DUX4L4[a]	NM_001177376	8,97E-03	-1,514
WDHD1	NM_007086	5,97E-04	-1,590	GABRA6	NM_000811	3,58E-03	-1,513
SUN2	NM_015374	2,49E-03	-1,586	L2HGDH	NM_024884	3,44E-03	-1,512
PHF10[a]	NM_018288	2,15E-03	-1,583	CDKN2C	NM_001262	1,50E-03	-1,511
SKA1	NM_001039535	4,42E-04	-1,576	ARHGAP19	NM_032900	1,78E-03	-1,510
CNTNAP3[a]	NM_033655	2,76E-04	-1,576	SLFN11	NM_001104587	5,13E-03	-1,508
RAD51[a]	NM_002875	2,80E-03	-1,575	C14orf80	NM_001134875	1,09E-03	-1,506
CDCA8	NM_018101	4,13E-04	-1,573	NCAPG	NM_022346	3,17E-03	-1,501

The genes containing a potential binding motif for E2F1 or NF-κB are respectively marked by 'a' and 'b'. The score of all marked genes was calculated by Pscan to be higher than the average matching score for all the promoters of the genome.

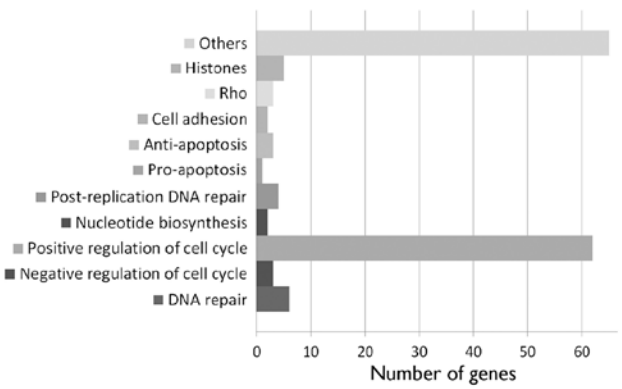

Figure 3. Number of downregulated genes in specific cellular processes 24 h after nickel ion irradiation (5 Gy). Almost half of the genes are involved in the positive regulation of the cell cycle. The referred processes were determined by search on the National Center for Biotechnology Information (NCBI) database.

Enrichment of transcription factor binding motifs. In order to identify the transcription factors potentially responsible for the differential gene expression upon irradiation, we scanned sequences close to the transcription start sites of these genes using Pscan (22). We found motifs for E2F1 among the transcription factor binding motifs enriched in the downregulated gene list, (p-value <10-19). On the other hand, we found two members of the REL family (RelA and NF-κB) with significantly enriched binding motifs in the list of upregulated genes (p-values <0.05).

Discussion

DNA damage persists 24 h after irradiation. We measured a significant increase in the number of γ-H2AX foci 2 h following nickel ion irradiation. This number was lower than the 30 spots per nucleus that we measured on average upon

Table II. List of the downregulated genes involved in cell cycle progression 24 h after 5 Gy of nickel ion irradiation.

DNA replication	Replication forks	Spindle	Kinetochore	Centromeres	Chromosome formation/stability
PRIM1	MCM6[a]	HAUS8	NDC80	PLK4	NCAPH
CDC6[a]	MCM7[a]	KIFC1	NUF2	MLF1IP	DDX11
DSCC1	MCM2[a]	NUSAP1[a]	SKA1	CEP55	PHF10[a]
ORC1	MCM5[a]	CDCA8		CENPH[a]	NCAPG2
POLA1[a]	MCM3[a]	KIF20A		CEP57L1	NCAPG
GINS2[a]	MCM10[a]	SKA1		CEP78	CDCA2
CDT1[a]	NFKBIL2	BUB1			
	RFC4	KIF2C			
		PRC1			
		BUB1B			
		KIF23			
		ESPL1			
		KIF11			

The genes containing a potential binding motif for E2F1 or NF-κB are marked by 'a'. The score of all marked genes was calculated by Pscan to be higher than the average matching score for all the promoters of the genome.

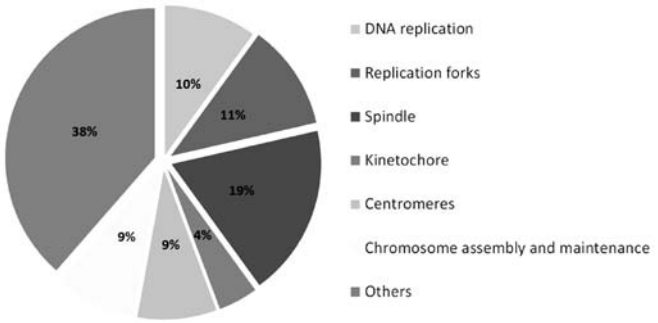

Figure 4. Pie chart representing proportions of genes downregulated 24 h after 5 Gy of nickel ion irradiation and involved in various processes of the cell cycle. Twenty-one percent of these genes play a role in DNA replication or in the replication forks and 41% play a role in the chromosome assembly and segregation (kinetochore, centromeres, spindle and chromosome).

X-irradiation with the same dose (data not shown). However, it is not so surprising since high LET irradiation deposits high amounts of energy along well-separated tracks. For nickel ions with a LET of 183 keV/μm and at a dose of 2 Gy, we calculated an average of 6.8 direct particle hits per nucleus (100 μm^2), which follows a Poisson distribution. However, we observed an average of 15 spots per nucleus. This may be due to the secondary radiation from the ion track and the basal level of endogenous γ-H2AX foci as observed in the controls.

Considering that the imaging of γ-H2AX foci was performed at the same angle as ion tracks produced by the irradiation beam, the complexity of the damage along these tracks could not be taken into account. However, the DNA damage complexity is known to be important in high LET irradiation (23-26). Although significantly increased, the γ-H2AX spot occupancy did not seem to be able to account for the complexity of DNA damage and showed similar results to the spot number measurement. This complex DNA damage is associated with slower repair (27) and therefore leads to a more pronounced delayed cellular damage (26). Our results revealed a significant level of γ-H2AX foci 24 h following nickel ion irradiation, as compared to controls; this suggests the presence of complex DNA damage.

Effects of high LET irradiation on the cell cycle. Nickel ion irradiation at a dose of 0.5 Gy elicited a lower gene expression response as compared to a dose of 5 Gy, in terms of the number of regulated genes and FC. At 24 h post-irradiation (5 Gy), we observed an upregulation of 12 genes involved in cell cycle arrest and a downregulation of 62 genes involved in cell cycle progression, among which were 3 members of the E2F transcription factor family (E2F1, E2F2 and E2F8). Moreover, the transcription factor binding motifs for E2F1 were found to be highly enriched in the list of downregulated genes. E2F is a family of transcription factors known to control G1- to S-phase transition (28), and to regulate the expression of a large variety of genes involved in DNA replication, DNA repair and apoptosis (29). Among the E2F transcription factors, E2F1 is known to be stabilized upon DNA damage through its phosphorylation by ataxia telangiectasia-mutated (ATM) kinase, ATM and Rad3-related (ATR) kinase and checkpoint kinase 2 (CHK2), as well as through its acetylation (29). Our results suggest a major role of E2F transcription factors in the response of EA.hy926 cells to high LET irradiation.

Six components of the minichromosome maintenance (MCM) complex, a heterohexamer helicase essential for the initiation and elongation step of DNA replication (30), were downregulated. This helicase may be a target for replication checkpoints (31), and is thought to be regulated mostly through post-transcriptional modifications (32). However, our results indicate a possible transcriptional regulation of several members of the MCM complex. Apart from MCM, many of the observed downregulated genes are involved in DNA replication and in chromosome formation, maintenance and segregation,

indicating their key role in cell cycle regulation in response to high LET radiation. Of note, we also reported the downregulation of 4 genes involved in post-replication DNA repair (UNG, UPF3A, MSH2 and MSH6), which may be silenced in the absence of active replication.

During this study, irradiation was performed on proliferating endothelial cells. The results gathered on cell cycle gene expression are therefore of moderate interest for mature blood vessels where proliferation is limited. However, as far as hadron therapy is concerned, our data indicate that high LET radiation may have a significant impact on the cellular proliferation of newly formed vascular vessels in the vicinity of the targeted tumor.

DNA damage response, oxidative stress and apoptosis. The expression of several genes involved in the DNA damage response, oxidative stress response and apoptosis was induced 24 h after 5 Gy of nickel ion irradiation, with a concomitant reduction of genes involved in DNA repair. However, these effects were not significant at a dose of 0.5 Gy, at either time points (8 and 24 h). These results suggest that a high dose of nickel ion irradiation induces a global DNA damage response, accompanied by cell cycle arrest and an increase in pro-apoptotic gene expression 24 h after irradiation.

Impact of radiation on genes related to cell adhesion. The impermeability of the endothelium is essential for the vasculature integrity and is determined by the cooperation of cell junctions and the cytoskeleton (33,34). In turn, adhesion molecules regulate cell homeostasis, growth and apoptosis (33). A number of cellular pathways are known to regulate cell adhesion in endothelial cells. These include growth factors, Rho GTPases, protein kinases and calcium signaling (34,35). The alteration of these pathways or of adhesion molecules may trigger the radiation-induced retraction observed by others in endothelial cells (13,14). Our study identified the differential expression of a number of genes known to be involved in cell adhesion (CEACAM1 and NEU1), cytoskeleton architecture (TUBA4A, LIMA1 and PLS1), Rho signaling (ARHGAP19, ARHGAP11B and RACGAP1) and calcium metabolism (ORAI3, CAMK2N1 and CALML4) 24 h after 5 Gy of nickel ion irradiation, which are potentially involved in endothelial cell retraction.

Expression of cytokines and chemokines. Inflammatory responses mediated by endothelial cells are believed to be involved in radiation-induced cardiovascular disease (7). Our study revealed the upregulation of 8 cytokines or chemokines that may be linked to inflammation (CXCL5, TGFA, TRIM22, TNFSF9, EBI3, IL-6, IL-11 and CD70). Of note, a search for transcription factor binding motifs that are significantly enriched in the list of upregulated genes upon 5 Gy of irradiation, revealed 2 members of the REL family (RelA and NF-κB). This family of transcription factors induces the expression of a multitude of genes, such as cytokines, proliferation, pro-survival and anti-apoptotic genes (36). For instance, we found IL-6 to be upregulated after 5 Gy of nickel ion irradiation. IL-6 expression was also shown to be upregulated by low-dose radiation therapy (10). IL-6 is known to be activated by NF-κB (36,37) and is thought to play a role in radiation-induced cardiovascular disease (1,7). The secretion of cytokines may also affect non-irradiated cells by a bystander effect. Indeed, in human fibroblasts, the external addition of IL-6 has been shown to increase γH2AX spot occupancy (38). The activation of NF-κB may be linked to the transcription factor, signal transducer and activator of transcription 3 (STAT3) (37), of which we also found significant binding motif enrichment.

In conclusion, we observed a downregulation of multiple genes involved in cell division, particularly at 24 h after nickel ion irradiation. Our results suggest an important role for E2F transcription factors in this process. The endothelial function being based on a plethora of intercellular interactions within a dynamic structure involving cell movements and turnover, cell cycle arrest may play a role in the radiation-induced cardiovascular disease. On the other hand, we observed an upregulation of various cytokines which may be induced by NF-κB. Other studies have also suggested that these cytokines may be linked to radiation-induced cardiovascular disease (10). The effects on gene expression were observed upon high doses of acute irradiation and are less relevant to space exploration. However, during hadron therapy, healthy tissues surrounding tumors, such as endothelial cells, may be subjected to high doses, which may lead to complications. In this study, we identified a multitude of potential molecular targets for further mechanistic studies out of which the gene expression changes upon high doses of nickel ion irradiation may be important for patients treated with hadron-therapy.

Acknowledgements

This study was supported by 4 PRODEX/BELSPO/ESA contracts (C90-303, C90-380, C90-391 and 42-000-90-380) and the ESA IBER-2 program. The authors wish to thank Professor Marco Durante for providing access to the GSI irradiation facilities.

References

1. Schultz-Hector S and Trott KR: Radiation-induced cardiovascular diseases: is the epidemiologic evidence compatible with the radiobiologic data? Int J Radiat Oncol Biol Phys 67: 10-18, 2007.
2. Blaber E, Marçal H and Burns BP: Bioastronautics: the influence of microgravity on astronaut health. Astrobiology 10: 463-473, 2010.
3. Brinckmann E (ed): Biology in Space and Life on Earth: Effects of Spaceflight on Biological Systems. WILEY-VCH Verlag GmbH & Co. KGaA, Weinheim, 2007.
4. Rong Y and Welsh J: Basics of particle therapy II biologic and dosimetric aspects of clinical hadron therapy. Am J Clin Oncol 33: 646-649, 2010.
5. Blakely EA and Chang PY: Biology of charged particles. Cancer J 15: 271-284, 2009.
6. Halle M, Hall P and Tornvall P: Cardiovascular disease associated with radiotherapy: Activation of nuclear factor kappa-B. J Intern Med 269: 469-477, 2011.
7. Hildebrandt G: Non-cancer diseases and non-targeted effects. Mutat Res 687: 73-77, 2010.
8. Rödel F, Frey B, Capalbo G, *et al:* Discontinuous induction of x-linked inhibitor of apoptosis in ea.Hy.926 endothelial cells is linked to NF-κB activation and mediates the anti-inflammatory properties of low-dose ionising-radiation. Radiother Oncol 97: 346-351, 2011.
9. Rödel F, Hofmann D, Auer J, *et al*: The anti-inflammatory effect of low-dose radiation therapy involves a diminished CCL20 chemokine expression and granulocyte/endothelial cell adhesion. Strahlenther Onkol 184: 41-47, 2008.

10. Rödel F, Keilholz L, Herrmann M, Sauer R and Hildebrandt G: Radiobiological mechanisms in inflammatory diseases of low-dose radiation therapy. Int J Radiat Biol 83: 357-366, 2007.
11. Rödel F, Schaller U, Schultze-Mosgau S, *et al*: The induction of TGF-beta(1) and NF-kappaB parallels a biphasic time course of leukocyte/endothelial cell adhesion following low-dose X-irradiation. Strahlenther Onkol 180: 194-200, 2004.
12. Ando K, Ishibashi T, Ohkawara H, *et al*: Crucial role of membrane type 1 matrix metalloproteinase (MT1-MMP) in Rhoa/Rac1-dependent signaling pathways in thrombin-stimulated endothelial cells. J Atheroscler Thromb 18: 762-773, 2011.
13. Kantak SS, Diglio CA and Onoda JM: Low dose radiation-induced endothelial cell retraction. Int J Radiat Biol 64: 319-328, 1993.
14. Onoda JM, Kantak SS and Diglio CA: Radiation induced endothelial cell retraction in vitro: correlation with acute pulmonary edema. Pathol Oncol Res 5: 49-55, 1999.
15. Gabrys D, Greco O, Patel G, Prise KM, Tozer GM and Kanthou C: Radiation effects on the cytoskeleton of endothelial cells and endothelial monolayer permeability. Int J Radiat Oncol Biol Phys 69: 1553-1562, 2007.
16. Pluder F, Barjaktarovic Z, Azimzadeh O, *et al*: Low-dose irradiation causes rapid alterations to the proteome of the human endothelial cell line EA.hy926. Radiat Environ Biophys 50: 155-166, 2011.
17. Grabham P, Hu B, Sharma P and Geard C: Effects of ionizing radiation on three-dimensional human vessel models: differential effects according to radiation quality and cellular development. Radiat Res 175: 21-28, 2011.
18. Takahashi Y, Teshima T, Kawaguchi N, Hamada Y, Mori S, Madachi A, Ikeda S, Mizuno H, Ogata T, Nojima K, Furusawa Y and Matsuura N: Heavy ion irradiation inhibits in vitro angiogenesis even at sublethal dose. Cancer Res 63: 4253-4257, 2003.
19. Kiyohara H, Ishizaki Y, Suzuki Y, Katoh H, Hamada N, Ohno T, Takahashi T, Kobayashi Y and Nakano T: Radiation-induced ICAM-1 expression via TGF-β1 pathway on human umbilical vein endothelial cells; comparison between X-ray and carbon-ion beam irradiation. J Radiat Res 52: 287-292, 2011.
20. Haberer T, Becher W, Schardt D and Kraft G: Magnetic scanning system for heavy ion therapy. Nucl Instrum Methods Phys Res A 330: 296-305, 1993.
21. De Vos WH, Van Neste L, Dieriks B, Joss GH and Van Oostveldt P: High content image cytometry in the context of subnuclear organization. Cytometry A 77: 64-75, 2010.
22. Zambelli F, Pesole G and Pavesi G: Pscan: finding over-represented transcription factor binding site motifs in sequences from co-regulated or co-expressed genes. Nucleic Acids Res 37: W247-W252, 2009.
23. Fokas E, Kraft G, An H and Engenhart-Cabillic R: Ion beam radiobiology and cancer: time to update ourselves. Biochim Biophys Acta 1796: 216-229, 2009.
24. Held KD: Effects of low fluences of radiations found in space on cellular systems. Int J Radiat Biol 85: 379-390, 2009.
25. Costes SV, Boissière A, Ravani S, Romano R, Parvin B and Barcellos-Hoff MH: Imaging features that discriminate between foci induced by high- and low-let radiation in human fibroblasts. Radiat Res 165: 505-515, 2006.
26. Blakely EA and Kronenberg A: Heavy-ion radiobiology: new approaches to delineate mechanisms underlying enhanced biological effectiveness. Radiat Res 150: S126-S145, 1998.
27. Chappell LJ, Whalen MK, Gurai S, Ponomarev A, Cucinotta FA and Pluth JM: Analysis of flow cytometry DNA damage response protein activation kinetics after exposure to x rays and high-energy iron nuclei. Radiat Res 174: 691-702, 2010.
28. Dyson N: The regulation of E2F by pRB-family proteins. Genes Dev 12: 2245-2262, 1998.
29. Biswas AK and Johnson DG: Transcriptional and nontranscriptional functions of E2F1 in response to DNA damage. Cancer Res 72: 13-17, 2012.
30. Costa A and Onesti S: The MCM complex: (just) a replicative helicase? Biochem Soc Trans 36: 136-140, 2008.
31. Forsburg SL: The MCM helicase: Linking checkpoints to the replication fork. Biochem Soc Trans 36: 114-119, 2008.
32. Chuang CH, Yang D, Bai G, Freeland A, Pruitt SC and Schimenti JC: Post-transcriptional homeostasis and regulation of MCM2-7 in mammalian cells. Nucleic Acids Res 40: 4914-4924, 2012.
33. Dejana E, Orsenigo F, Molendini C, Baluk P and McDonald DM: Organization and signaling of endothelial cell-to-cell junctions in various regions of the blood and lymphatic vascular trees. Cell Tissue Res 335: 17-25, 2009.
34. Prasain N and Stevens T: The actin cytoskeleton in endothelial cell phenotypes. Microvasc Res 77: 53-63, 2009.
35. Bogatcheva NV and Verin AD: The role of cytoskeleton in the regulation of vascular endothelial barrier function. Microvasc Res 76: 202-207, 2008.
36. Oeckinghaus A and Ghosh S: The NF-kappaB family of transcription factors and its regulation. Cold Spring Harb Perspect Biol 1: a000034, 2009.
37. Karin M: NF-kappaB as a critical link between inflammation and cancer. Cold Spring Harb Perspect Biol 1: a000141, 2009.
38. Dieriks B, De Vos WH, Derradji H, Baatout S and Van Oostveldt P: Medium-mediated DNA repair response after ionizing radiation is correlated with the increase of specific cytokines in human fibroblasts. Mutat Res 687: 40-48, 2010.